PPS
www.rsc.org/pps

A concept for G protein activation by G protein-coupled receptor dimers: the transducin/rhodopsin interface

Slawomir Filipek,*[a] Krystiana A. Krzysko,[a,b] Dimitrios Fotiadis,[c] Yan Liang,[d] David A. Saperstein,[d] Andreas Engel[c] and Krzysztof Palczewski[d,e,f]

[a] *International Institute of Molecular and Cell Biology, Warsaw, PL-02109, Poland*
[b] *Faculty of Chemistry, Warsaw University, Warsaw, Poland*
[c] *M.E. Müller Institute for Microscopy, Biozentrum, University of Basel, CH-4056 Basel, Switzerland*
[d] *Department of Ophthalmology, University of Washington, Seattle, WA 98195, USA*
[e] *Department of Pharmacology, University of Washington, Seattle, WA 98195, USA*
[f] *Department of Chemistry, University of Washington, Seattle, WA 98195, USA*

Received 4th December 2003, Accepted 4th February 2004
First published as an Advance Article on the web 27th February 2004

G protein-coupled receptors (GPCRs) are ubiquitous and essential in modulating virtually all physiological processes. These receptors share a similar structural design consisting of the seven-transmembrane α-helical segments. The active conformations of the receptors are stabilized by an agonist and couple to structurally highly conserved heterotrimeric G proteins. One of the most important unanswered questions is how GPCRs couple to their cognate G proteins. Phototransduction represents an excellent model system for understanding G protein signaling, owing to the high expression of rhodopsin in rod photoreceptors and the multidisciplinary experimental approaches used to study this GPCR. Here, we describe how a G protein (transducin) docks on to an oligomeric GPCR (rhodopsin), revealing structural details of this critical interface in the signal transduction process. This conceptual model takes into account recent structural information on the receptor and G protein, as well as oligomeric states of GPCRs.

Introduction

G protein-coupled receptors (GPCRs) constitute one of the largest gene families.[1–3] These receptors are similar in their overall topology, which consists of seven-transmembrane α-helical segments, the ligand binding site located at the extracellular region or within the transmembrane α-helical bundle, and the intracellular region that is responsible for coupling to G proteins and other proteins.[4] The most extensively studied GPCR is rhodopsin.[5] It is expressed in rod photoreceptor cells (Fig. 1A) which are involved in scotopic vision.[6] In addition to the plasma membrane, rhodopsin resides in the intracellular membranes that form stacks of flattened discs in the rod outer segment (ROS), the subcellular compartment dedicated to phototransduction (Fig. 1B). Upon activation by light, the chromophore within the transmembrane segment of rhodopsin undergoes photoisomerization, triggering a conformational change in the surrounding polypeptide chain.[7,8]

Rhodopsin is the only GPCR for which a crystal structure has been determined[9,10] but it is believed that other receptors from the GPCR superfamily have similar three-dimensional structures.[11] Importantly, the structure of several G protein subtypes[12–19] is highly conserved (reviewed in ref. 20). Moreover, the crystal structures of arrestins,[21–23] molecules that quench the activity of GPCRs,[24] are also highly conserved (reviewed in ref. 20). Different GPCRs can activate the same G protein subtype, and similarly, one GPCR can couple to different G protein subtypes at least *in vitro*. In addition, the mechanism of receptor activation appears to be conserved for all members of the GPCR superfamily.[3,8,25] These findings suggest that the productive coupling between different GPCRs and G proteins (or arrestins) is mechanistically analogous.

In this work, we present a simple model of G protein activation that considers the size of partner proteins, structural constraints, and organization of GPCRs in the membranes. We do not intend to summarize the large amount of data accumulated over decades, but rather to describe a model that utilizes recent structural information. Our model reveals structural details about this critically important interface between a

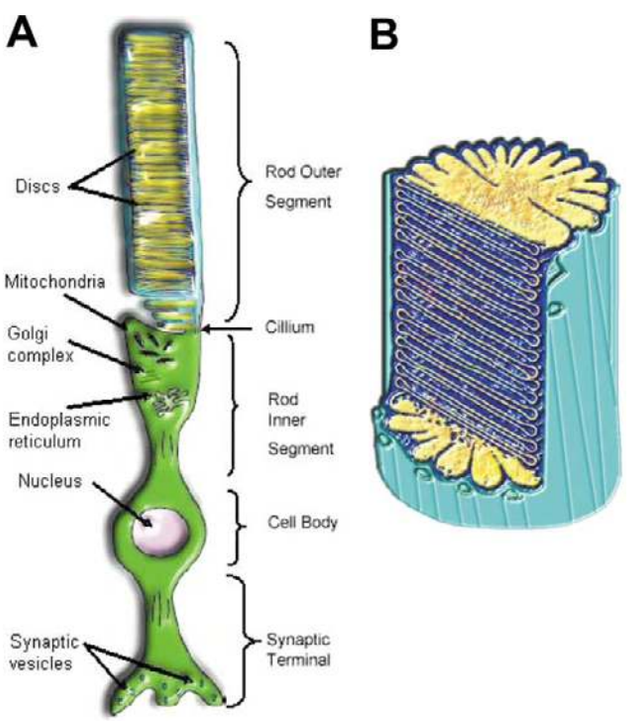

Fig. 1 Diagram of the retinal rod photoreceptor cell. (A) The major elements of highly differentiated rod photoreceptor cells are labeled. Adapted from ref. 5. (B) The stack of internal disc membranes (yellow) within the rod outer segment (ROS) enveloped by the plasma membranes (navy blue; adapted from Brown *et al.*[83]). The disc membrane contains ~3 mM rhodopsin (red).

DOI: 10.1039/b315661c

GPCR (rhodopsin) and a G protein (transducin, Gt) involved in the first amplification gain in the signal transduction cascade.

Methods

Molecular model of the rhodopsin oligomer

Our current model of the rhodopsin dimer, the so called "IV–V model" where the dimeric interface is formed between helices IV and V[38,39] is based on the 1N3M model of rhodopsin oligomer deposited in the Protein Data Bank (PDB). The foundation for this model was the crystal structure of rhodopsin deposited under the 1HZX identifier in the PDB. In the crystal, rhodopsin formed a dimer where one rhodopsin is rotated by ~170° relative to the second molecule, thus only a monomer of rhodopsin was used in the modeling. Missing residues in the loop connecting helices V and VI were modeled with the Discover program (InsightII 2000, Accelrys Inc.). Based on the AFM measurements of distances between rhodopsins in the paracrystal, a model was assembled where helices IV and V form an interface between rhodopsin monomers. Energetic considerations together with geometrical constraints obtained from AFM excluded other models of the oligomeric structures. Oligomers in our model (1N3M) are built from separate dimers and linked together by a long loop between helices V and VI. A dimer is a repetitive motif in the oligomer (double row), therefore tetramers and higher structures are connected in the identical manner as dimers. Current simulations were carried out using the CVFF force field (Discover, InsightII 2000, Accelrys Inc.). Atomic charges were determined in the Discover program by minimizing the electrostatic energy of the system while charges were variable. Series of short molecular dynamics simulations, up to 100 ps in a single run, were used to build a reliable system of interacting proteins. After each molecular dynamics run, optimization of the whole structure was performed (maintaining frozen parts when necessary). Similar procedures were used previously to model rhodopsin mutants.[42]

The 1N3M model was improved by the addition of phospholipids. Specifically, three types of phospholipids were used with phosphatidylcholine headgroups on the intradiscal side and phosphatidylethanolamine and phosphatidylserine headgroups (three times more phosphatidylethanolamine headgroups than phosphatidylserine) on the cytoplasmic side.[43,44] All three types of phospholipids contain the saturated stearoyl chain (18 : 0) in the *sn*1 position and the polyunsaturated docosahexaenoyl chain (22 : 6) in the *sn*2 position. Phospholipids were inserted between rhodopsin monomers and the complex was optimized by molecular dynamics followed by energy minimization with the rhodopsin monomers frozen in their initial positions. Next, the complex of six rhodopsin monomers was subjected to several steps of short molecular dynamics simulations followed by energy minimization to remove disallowed contacts. Favorable interactions between inserted or modified subunits were created usually during the first 10 ps of molecular dynamics simulation. The distances between the rhodopsin monomers in the paracrystal remained unchanged after addition of the phospholipids and optimization of the model without any constraints. Cholesterol and water molecules were not included in the model.

Modeling of Gt and the Gt–rhodopsin oligomer complex

Bovine heterotrimeric Gt was built from the crystal structure of truncated Gt (1GOT),[15] by homology modeling (Modeler in InsightII 2000, Accelrys Inc.). Missing residues 1–5 of Gt_{α}, residues 1–8 of Gt_{γ}, and residues 67–74 of Gt_{γ} were added and the resulting structures were optimized by molecular dynamics. The missing residues 344–350 of the C-terminal region of Gt_{α} responsible for the recognition of activated rhodopsin[45] was built based on the NMR structure of the 11-residue fragment deposited in the Protein Data Bank (1AQG).[46] The C-terminal helix in 1GOT is terminated and 1AQG starts with this helix allowing both helical parts to be partially superimposed to preserve the axis of the shared part of the C-terminal helix. Subsequent optimizations were performed for the complex of heterotrimeric Gt after binding to the rhodopsin oligomer.

After modeling of all missing termini in heterotrimeric Gt, Gt_{α} was docked onto rhodopsin dimer where one molecule was activated by movement and rotation of H-VI, followed by slight movements of neighboring helices to accommodate changes in the structure. The least amount of tension was achieved during docking of the C-terminal region of Gt_{α} along the longest primary axis of activated rhodopsin. Docking was continued until the N-terminal helix of Gt_{α} (parallel to the cytoplasmic surface of the rhodopsin dimer) interacted firmly with the cytoplasmic cavities of adjacent inactive rhodopsin in the dimer. Next, β- and γ-subunits were added, obtained from the crystal structure of Gt,[15] and the whole complex was optimized by energy minimization. Short molecular dynamics runs of 5–10 ps were applied to different parts of the model to assure proper interactions between molecules in the complex. A longer molecular dynamics run (100 ps) was performed to validate that the complex is stable.

Justification of models

Computational methods allowed creating protein complexes at the atomic level. To generate the model, we used the crystal structure of the rhodopsin monomer with one loop modeled in and a hybrid structure of Gt based on the crystal structure of the protein core and the NMR structure of a peptide fragment. The IV–V model of the rhodopsin dimer used in the 1N3M model of the rhodopsin oligomer with added phospholipids is supported by the AFM data and energetic considerations. The terminal regions of Gt_{α} and Gt_{γ} are not seen in the crystal of Gt (1GOT) because they are unstructured. The C-terminal region of Gt_{α} (determined by NMR) was linked with the appropriate end of the α subunit based on the alignment of identical residues in both structures. Other termini missing in the crystal structure were modeled as described above. This model was not confirmed by structural methods.

The quality of the model was evaluated based on the computational considerations. From the theoretical point of view, the correct structure is characterized by the lowest energy. However, this supposition may lead to many structures with a similar energy. Furthermore, the parameters of the force field, especially atomic charges, significantly affected the calculated energy of the complex. The CVFF force field, which is suitable for proteins, was used and atomic charges were obtained by allowing partial charge polarization. Involvement of water in calculations requires very long runs of molecular dynamics to obtain a stable, low energy system. Owing to the dimensions of the model such calculations were not feasible, and therefore precise calculation of differences in energy between considered models was not possible. Instead, we used the following criteria in the model building: (1) larger contact surface between interacting parts leads to a more stable complex; and (2) preorganization of the rhodopsin cytoplasmic surface facilitates Gt binding and stabilization of the whole complex.

Functional forms of GPCRs: oligomers, dimers, and monomers

GPCRs can form dimers and oligomers (reviewed in ref. 4, 26–36). Support for the oligomerization of GPCRs, along with dimerization, has been obtained experimentally by co-immunoprecipitation, energy transfer between two tagged receptors, disulfide cross-linking, pharmacological enhancement of the signal arising from one receptor by the agonist of

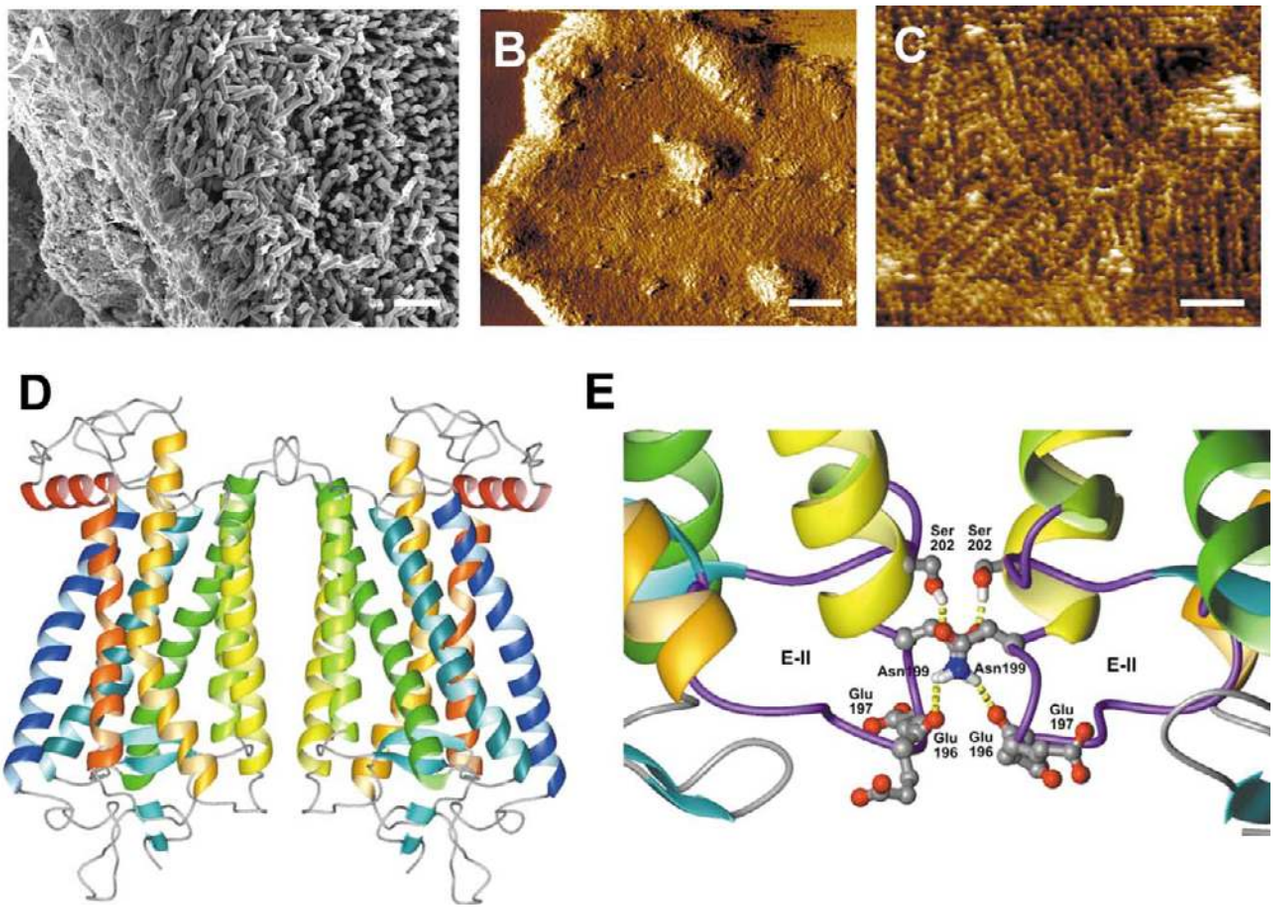

Fig. 2 Visualization and modeling of elements of the rod outer segment (ROS). (A) Scanning electron micrograph of isolated mouse retina (see ref. 38 for methods). The ROS are projecting toward the viewer. Scale bar 10 μm. (B) AFM deflection image of an open, spread-flattened disc from ROS. Scale bar 50 nm. (C) Higher magnification of the disc membrane imaged by AFM showing rows of rhodopsin dimers (see ref. 37–39 for methods). Scale bar 25 nm. (D) Model of the rhodopsin dimer (from ref. 38 and 39). Helices are color coded from blue (helix I, H-I) to red (cytoplasmic H-8), as in the spectrum of visible light. Contacts between monomers involve loops between H-III and H-IV at the cytoplasmic side, helices H-IV (light green) and H-V (green) in the transmembrane segment and loops between H-IV and H-V at the extracellular (intradiscal) side. (E) Hydrogen bond interactions between the E-II loops formed between H-IV (light green) and H-V (yellow) in the rhodopsin dimer. This extracellular loop E-II is colored in purple. Intermolecular contacts are formed by Asn^{199} and Ser^{202} of both monomers, as described in the text.

the second receptor in the heterodimeric complex, radiation inactivation, gel exclusion chromatography, and interference with intracellular trafficking.

To determine the functional oligomerization state of rhodopsin, we have used freshly isolated, fully functional murine discs isolated from ROS (Fig. 2A) that were characterized by biophysical and biochemical methods and subjected to electron microscopy (EM) and atomic force microscopy (AFM).[37–39] The size and shape of single-layered disc membranes after osmotic bursting are compatible with those of double-layered, intact discs imaged by AFM and observed by EM using thin sections of the mouse retina and isolated ROS. AFM of murine disc membranes adsorbed on freshly cleaved mica (Fig. 2B) revealed distinct rows of dimers organized in paracrystalline lattices (Fig. 2C). Paracrystalline packing of rhodopsin was also evident when disc membranes were analyzed by EM. Hence, the observation of crystalline packing was independent of the support, *i.e.*, mica, carbon film and another disc membrane.[38–40] Recently, the results mentioned above on the oligomeric organization of rhodopsin in native disc membranes were challenged by Chabre, Cone and Saibil,[41] and their comments were answered by us with additional experiments.[39,40] The experimental data from AFM together with the crystallographic data on the rhodopsin structure allowed us to build a semi-empirical molecular model for the rhodopsin paracrystal with a dimer as a structural unit (Fig. 2D). A comparison of the current molecular models for GPCR oligomers in biological membranes has been previously discussed.[39]

Molecular model of rhodopsin in native disc membranes

The model of a rhodopsin tetramer embedded in the membrane is shown in Fig. 3A and B. The structure of the model membrane is uniform throughout. However, *in vivo*, ROS membranes are not necessarily uniform throughout and may contain islands of membrane/protein rafts.[47–50] Intradimeric interactions between the extracellular loop E-II that connects H-IV and H-V (Fig. 2E; dashed yellow lines) may facilitate communication between rhodopsin molecules forming the dimer. Such interactions at the extracellular side of GPCRs may respond to changes upon ligand binding or upon photoisomerization of the chromophore in the case of rhodopsin. Two monomers of rhodopsin interact with each other at the extracellular (intradiscal) side, at the cytoplasmic side (loop between H-III and H-IV, and the C-terminal regions), and also within the transmembrane helices (H-IV and H-V). Only the extracellular interactions involving loop E-II can transmit information about ligand binding from one receptor monomer to another because of the close proximity of E-II to the ligand binding pocket. This region contains a disulfide bridge involving residues Cys^{110} and Cys^{187} (ref. 3 and 51), which are highly conserved among most of the GPCRs.[5,11] Rhodopsin monomers are bridged at the extracellular side by hydrogen bonds between Ser^{202} and Asn^{199}. Asn^{199} extends the hydrogen bond network even further to Glu^{196}. Additionally, an adjacent Glu^{197} residue points its carbonyl oxygen atom toward Asn^{199}, contributing to the bridging of the two receptor monomers.

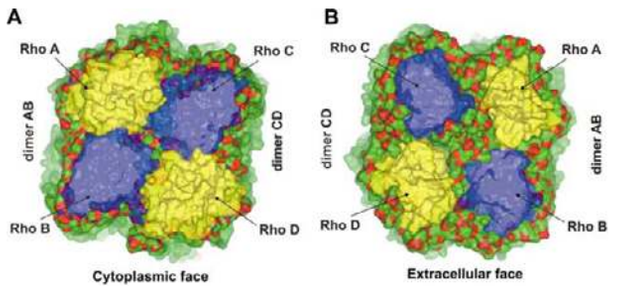

Fig. 3 Rhodopsin tetramer surrounded by phospholipids. View from the cytoplasmic (A) and extracellular sides (B). Phospholipids are colored by the atom type (carbon in green, oxygen in red, nitrogen in blue); rhodopsin monomers are in yellow and blue to differentiate between them. Rhodopsin surfaces are partially transparent to visualize the phospholipids. Although interacting rhodopsins form the contiguous surface, phospholipids are also located beneath rhodopsin cytoplasmic loops. The extracellular surface of rhodopsin is much smaller and phospholipids are clearly visible between rhodopsin dimers.

This hydrogen bond is formed and broken during the course of molecular dynamics simulation. The second extracellular loop of the dopamine D2 receptors is also a part of the binding-site similarly to E-II of rhodopsin.[52] Thus, this mechanism of communication between receptors through E-II in the dimer may extend to other GPCRs as well.

The distance between rhodopsin monomers in a dimer is 3.8 nm, which is also the distance to the closest rhodopsins in adjacent dimers. The main axis of rhodopsin is tilted by 5° in relation to the vector perpendicular to the membrane and also 5° in relation to each other in the paracrystal. Double rows of rhodopsins (visible in Fig. 2C) are located every 8.4 nm. Based on the distance between two rhodopsins from two double rows, it appears that these rhodopsins are located too far away to interact concurrently with a single Gt molecule. Therefore, the 1N3M model was truncated at the double row boundary for investigating interactions with Gt. The whole 1N3M model was used only for a preliminary calculation of Gt diffusion in the membranes (*via* farnesyl or geranylgeranyl bound to the C-terminus of G_γ subunits of the G proteins). Up to three highly mobile phospholipids in a row can fit between rhodopsin molecules from adjacent double rows (data not shown). Therefore, even in the rhodopsin paracrystal, the inter-row space allows for the movement of heterotrimeric Gt along rows of rhodopsin dimers. However, there is no space between dimers at the cytoplasmic side to allow Gt to enter (Fig. 3A). At the extracellular side (Fig. 3B), a row one phospholipid wide is present between dimers. Apart from sugar groups, the extracellular domains do not interact, allowing movement of rhodopsin at this side of the dimer. Tilting of the dimer can facilitate Gt binding at the cytoplasmic side and the recognition of activated rhodopsin by the C-terminal region of Gt_α.

The calculated total flat surface area, defined as the area projected into the *x–y* plane, of the rhodopsin tetramer surrounded by a single phospholipid row (Fig. 3B) viewed from the extracellular side is 79 nm²; protein and lipid components have surface areas of 47 nm² and 32 nm² (40%), respectively. Viewed from the cytoplasmic side (Fig. 3A), the total flat surface area is 76 nm², including protein (55 nm²) and lipid components [21 nm² (27%)]. The difference between the extracellular and the cytoplasmic total flat surface area is a result of the number of phospholipids residing at both sides and the different packing forces. As a consequence of the compact N-terminal cap[9,10] the protein component at the extracellular side is 8 nm² smaller than the protein component on the cytoplasmic surface. The C-I, C-II and C-III loops and the C-terminal region contribute to the extended protein surface on the cytoplasmic side. The C-II and C-III loops and the C-terminal region form a broad platform bridging dimers.

The thickness of the membrane (calculated as a distance between phosphorus atom layers at the cytoplasmic and extracellular sides) is 4.1 nm. Approximately 120 phospholipids can fit between rhodopsin monomers and wrap the rhodopsin tetramer within a lipid bilayer. On average, this envelope increases the surface contours of the oligomer model by 0.8 nm. The AFM experiments yielded a lipid bilayer thickness of 3.7 ± 0.2 nm, while single-layered disc membranes[38] were 7–8 nm thick; rhodopsin protruded by 1.4 ± 0.2 nm out of the lipid bilayer on the cytoplasmic side.[37] Since rhodopsin is an ellipsoid with the longest dimension of ~7.5 nm,[10] the theoretical calculations, structural data and AFM data are compatible with each other. Chemical analysis of the phospholipid and rhodopsin contents in mouse, rat and bovine ROS revealed a molar ratio of 54 : 86 for phospholipids : rhodopsins.[53,54] Based on our model,[38] the maximal density of rhodopsin is ~60 000 per μm². Because the average density of rhodopsin is ~40 000 per μm² and one rhodopsin displaces ~40 phospholipids in the lipid bilayer, the calculated molar ratio is ~65 phospholipids to one rhodopsin and our model is in agreement with chemical analysis of phospholipids in ROS.

G protein structure

The G protein of the visual system (transducin, Gt) is a heterotrimer consisting of α, β and γ subunits. The Gt_α subunit is subdivided into two distinct domains. The GTPase domain contains a six-stranded β-sheet surrounded by six α-helices. The helical domain has a long central helix surrounded by five shorter helices. The N-terminal region consists of a long α-helix pointing out from the rest of the Gt_α subunit (Fig. 4). GDP is bound to a cleft between the GTPase and helical domains. Both domains have almost identical structures in the GTP and GDP-bound state. Significant changes are observed within the GTPase domain contacting $Gt_{\beta\gamma}$[14,15,55] (reviewed in ref. 56 and 57). The Gt_β subunit has a long N-terminal helix followed by a repeating module of seven β-sheets, each with four antiparallel strands, forming the β-propeller structure. The Gt_γ subunit contains two helices. The N-terminal helix interacts with the N-terminal helix of Gt_β, whereas the remaining polypeptide chain of Gt_γ interacts with the β-propeller structure of Gt_β.[15] No interactions were observed between α- and γ-subunits in the crystal structure (1GOT) (Fig. 4A, B), because the Gt_β separates these subunits. With reconstruction of the missing parts of Gt, the N-terminus of Gt_α and the C-terminus of Gt_γ move toward each other and the proper shape of C-terminus of Gt_γ is formed as a consequence of the interactions with the C-III loop of rhodopsin. The N-terminal region of the Gt_γ subunit points to the cleft between the GTPase and helical domains of Gt_α (Fig. 4B).

Mechanism of G protein docking on the GPCR

Coupling of Gt requires that rhodopsin is activated, and for effective binding, all three subunits of Gt are required. This is accomplished by a ~90° rotation of H-VI (Fig. 5, colored orange). This event is possible because photoactivation of rhodopsin leads to the breaking and establishing of interactions between the D(E)RY region of H-III and H-VI.[5,42] In addition, some adjustment occurs within H-VII and H-8. Gt binds to the cytoplasmic surface of photoactivated rhodopsin. Formation of the productive complex between photoactivated rhodopsin and Gt leads to GDP dissociation. The binding of GTP to the complex induces dissociation of Gt_α-GTP and $Gt_{\beta\gamma}$ subunits.

After modeling of all of the missing termini in heterotrimeric Gt, Gt_α was docked to the rhodopsin dimer where one molecule was activated by movement and rotation of H-VI, followed by slight movements of neighboring helices to accommodate changes in the structure (Fig. 5). The least amount of tension was achieved during docking of the C-terminal region of Gt_α along the longest primary axis of activated rhodopsin. Docking

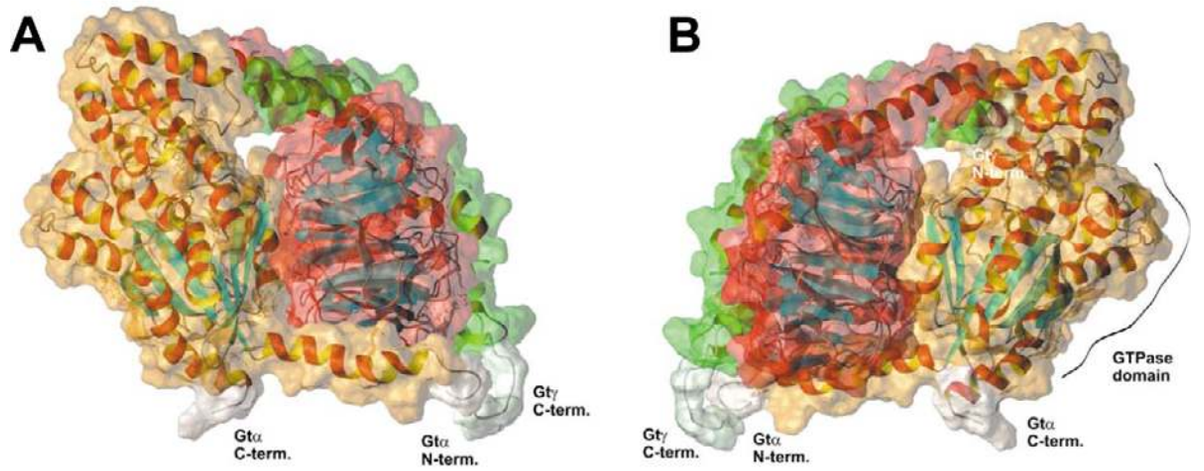

Fig. 4 Ribbon structure of $Gt_{\alpha\beta\gamma}$ in the conformation capable to form a complex with the rhodopsin dimer. Surfaces are colored according to subunits: α – orange, β – red, γ – green. The modeled missing fragments are labeled and colored with light orange (both termini of Gt_α) and light green (both termini of Gt_γ). (A) Assembly of Gt subunits. Gt_α is facing viewer. (B) Gt after rotation by 180° around vertical axis.

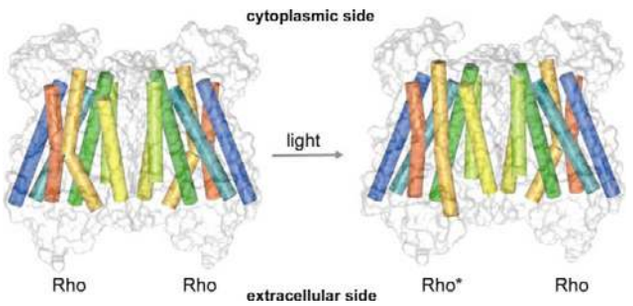

Fig. 5 Model of activation of the rhodopsin dimer. Activation of only one rhodopsin monomer is necessary to bind and activate Gt. Transmembrane helices shown as cylinders colored from blue (H-I) to red (H-VII). During activation, H-VI (orange) is rotated about 90° and its cytoplasmic end is moved out of the rhodopsin center. H-VII (red) accommodates to these changes.

was continued until the N-terminal helix of Gt_α (parallel to the cytoplasmic surface of the rhodopsin dimer) interacted firmly with the cytoplasmic cavities of adjacent inactive rhodopsin in the dimer. The Gt–rhodopsin complex covers four rhodopsin molecules (Fig. 6A–C, and Fig. 7). The long N-terminal helix of Gt_α divides the cytoplasmic part of the second rhodopsin in the middle. One half is occupied by the C-terminal region of rhodopsin and the second half by loops C-II (between helices H-III and H-IV) and C-III (between helices H-V and H-VI). In particular, the C-terminal region of Gt_γ is separated from the N-terminal region of Gt_α by the C-III loop of rhodopsin. Fig. 7 also shows the location of the farnesylated C-terminus of Gt_γ and the palmitoyl chains of rhodopsin at Cys^{322} and Cys^{323}. They interact closely with each other and fit smoothly into the lipid bilayer. The C-terminal region of Gt_γ passes between rhodopsin molecules from different dimers (visible on Fig. 6B with different tints of blue indicating rhodopsin molecules). The transparent surfaces of rhodopsin molecules (Fig. 8A) illustrate how deep the C-terminal region of Gt_α is inserted (yellow rhodopsin) and also how the N-terminal region of Gt_α interacts with the cytoplasmic loops of another rhodopsin (blue). Fig. 8B shows the coverage of the cytoplasmic part of the rhodopsin dimer by Gt_α. Next, β- and γ-subunits were added, obtained from the crystal structure of Gt,[15] and the whole complex was optimized by energy minimization. Short molecular dynamics runs of 5–10 ps were applied to different parts of the model to assure proper interactions between molecules in the complex. A longer molecular dynamics run (100 ps) validated that the complex is stable. All optimizations and molecular dynamics simulations were performed employing InsightII 2000 (Accelrys Inc.).

The interface between Gt and photoactivated rhodopsin

The contact area between Gt and rhodopsin is extensive in our model. The major interactions with rhodopsin are formed by Gt_α, and the other subunits have to comply with the overall Gt conformation. The interaction between Gt_α involves, in partic-

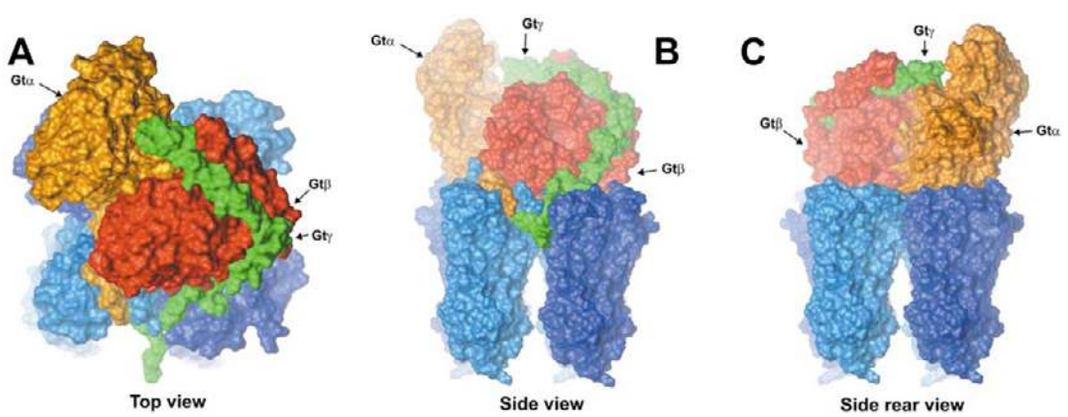

Fig. 6 Model of two rhodopsin dimers with one heterotrimeric Gt. (A) View from the cytoplasmic side. Rhodopsin molecules are colored in blue, Gt_α in orange, Gt_β in red, and Gt_γ in green. Gt occupies two rhodopsin dimers, with only one rhodopsin molecule needing to be activated. (B) Side view of the complex between oligomeric rhodopsin and Gt. In the foreground, β- and γ-subunits together with the N-terminal region of Gt_α (orange) and the C-terminal region of Gt_γ (green). (C) Side rear view of the complex between oligomeric rhodopsin and heterotrimeric Gt. In the foreground, α- and β-subunits of Gt are visible.

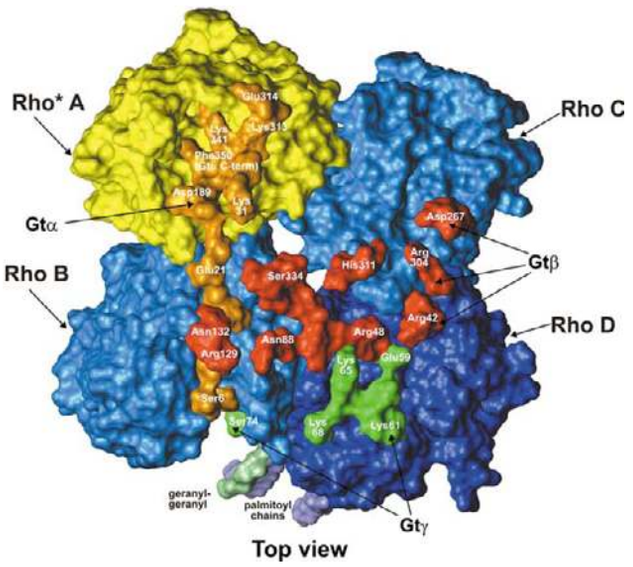

Fig. 7 Closer view of the interactions between heterotrimeric Gt and the rhodopsin tetramer (dimers denoted A–B and C–D). View from the cytoplasmic side shows only those residues of α- (orange), β- (red) and γ-subunits (green) of Gt that interact with rhodopsin. Activated rhodopsin is shown in yellow. Other rhodopsin molecules are colored in different tints of blue to facilitate identification of rhodopsin monomers. A detailed list of interactions between Gt and rhodopsin molecules is given in Table 1.

ular, monomer A (see figure legend to Fig. 7) with an interacting surface of 18.6 nm² and monomer B (11.7 nm²). Subunit Gt_β interacts with four rhodopsin monomers (A–D), the interfaces being 0.7 nm² with subunit A, 4.9 nm² with B, 5.9 nm² with C and 7.1 nm² with D. Subunit Gt_γ forms an interface only with monomers B (2.9 nm²) and D (7.8 nm²). The complex of Gt with the activated rhodopsin oligomer is stable during energy optimization and the interacting surfaces are well defined.

Gt_α binds to photoactivated rhodopsin through hydrogen bonds as well as ionic and hydrophobic interactions (see Table 1). They involve all of the cytoplasmic loops and the C-terminal region of rhodopsin, forming several bond interactions. The contact sites also involve tips of H-III, H-VI, which are the two longest helices of rhodopsin, and the cytoplasmic H-8. The D(E)RY motif located at the cytoplasmic end of H-III,[5] involved in the activation process of rhodopsin, is engaged in the interaction with the C-terminal region of Gt_α. These residues are mainly hydrophobic but can also form hydrogen bonds with their peptide bonds. Interactions of the N-terminal region of Gt_α with the second rhodopsin molecule are formed mainly with C-I, C-II, the C-terminal region, and H-VI of monomer B and involve hydrophilic as well as six ionic interactions (Table 1). Gt_β forms only hydrogen bonds with rhodopsin monomers B and C, and four ionic interactions with monomer D exist (C-II loop and C-terminal region of rhodopsin). Gt_γ forms hydrogen bonds with rhodopsin monomers B and D, with two ionic interactions (the C-I loop and the C-terminal region of rhodopsin). These interactions provide a temporary anchor and can be replaced with water when $Gt_{\beta\gamma}$ dissociates.

Fig. 9A–C shows the preorganization of the cytoplasmic loops in the rhodopsin dimer and the subsequent binding of Gt. Even without Gt, the deep cavities at the cytoplasmic side are evident (Fig. 9A). The longest cavity dividing rhodopsin in the middle is created by the C-terminal region (forming one side of this cavity) and the long C-III loop (forming the other side). These cavities are connected, creating a long canyon across the dimer. Fig. 9B shows the complex between Gt and a rhodopsin dimer. For clarity, only the N- (orange) and C-terminal regions (yellow) of Gt_α are shown. Both termini are formed by single

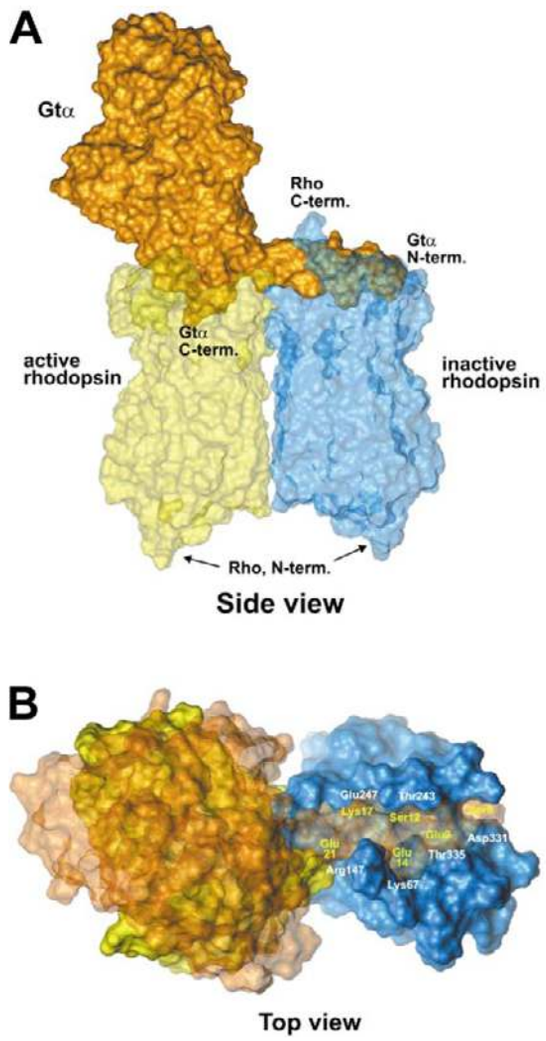

Fig. 8 Complex between the rhodopsin dimer and Gt_α. (A) Side view of the complex. Both rhodopsin molecules are transparent to show details of binding. Activated rhodopsin is shown in yellow. (B) Top view of the complex. The surface of Gt_α is transparent to visualize the rhodopsin shape. Interacting residues are shown on the N-terminal helix of Gt_α and inactive rhodopsin – activation of both rhodopsin monomers is not necessary for binding of Gt. Yellow and white labels denote Gt_α and rhodopsin residues, respectively.

helices. The N-terminal helix lies parallel to the cytoplasmic surface of rhodopsin while the C-terminal region penetrates deep into the rhodopsin core. For proper Gt binding, the activation of rhodopsin monomer A is required. Locations of rhodopsin helices in relation to the helical termini of Gt_α are shown in Fig. 9C. The C-terminal region of Gt_α is located between rhodopsin helices H-II, H-III, H-VI and H-VII.

Mutational and cross-linking studies have provided experimental data identifying residues in Gt and rhodopsin that are in close proximity. Acharya *et al.*[58] identified Tyr^{136}–Val^{139} in H-III of rhodopsin as interaction sites with Gt. Khorana's group[59,60] has shown that Leu^{19}–Arg,[28] Arg^{310}–Lys^{313} and Glu^{342}–Lys^{345} of Gt_α are cross-linked to $Ser^{240}Cys$ in the C-III loop of light activated rhodopsin. The Asn^{310}–Gln^{312} region (H-8) interacts with residues 340–350 of Gt_α.[61,62] In addition to the C-terminal region,[45] the N-terminal part of Gq/11α contains a region involved in the recognition of different GPCRs.[63] As noted before, a simple model of a 1 : 1 rhodopsin–Gt interaction is not compatible with observations from structural studies, whereas the dimer or higher order crystalline structure of rhodopsin provides a platform that can anchor both the α- and βγ-subunits of Gt.[64] Indeed, Baneres and Parello[65] found evidence of a pentameric assembly between dimeric leukotriene B4 receptor BLT1 and heterotrimeric Gi.

Table 1 Interactions of Gt with two rhodopsin dimers and between two Gt_{α}s[a]

	Gt_{α}	–	Rho*[b] (molecule A)
Ionic			
	Asp189	–	Lys141 (C-II)
	Lys341	–	Asp331 (C-term)
	Lys341	–	Glu332 (C-term)
	Glu342	–	Lys67 (C-I)
	Asp346	–	Lys67 (C-I)
H-bonds			
	Arg28	–	Ser144 (C-II)
	Lys31	–	Pro347 (C-term)
	Lys31	–	Ala348 (C-term)
	Thr215	–	Ala346 (C-term)
	Lys313	–	Ser334 (C-term)
	Glu314	–	Ala333 (C-term)
	Lys341	–	Glu332 (C-term)
	Glu342	–	Thr336 (C-term)
	Lys345	–	Lys67 (C-I)
	Asp346	–	Ala346 (C-term)
	Phe350	–	Thr70 (H-II)
	Leu349	–	Arg135 (H-III)
	Phe350	–	Gln312 (H-8)
Hydrophobic			
	Leu349	–	Phe148 (C-II)
	Phe350	–	Leu72 (H-II)
	Phe350	–	Val250 (H-VI)

	Gt_{α}	–	Rho (molecule B)
Ionic			
	Arg13	–	Glu247 (H-VI)
	Glu14	–	Lys67 (C-I)
	Glu16	–	Lys141 (C-II)
	Lys17	–	Glu247 (H-VI)
	Glu21	–	Arg147 (C-II)
	Glu24	–	Arg147 (C-II)
H-bonds			
	Gly2	–	Lys245 (H-VI)
	Ser6	–	Asp331 (C-term)
	Glu9	–	Thr335 (C-term)
	Ser12	–	Thr243 (H-VI)
Hydrophobic			
None			

	Gt_{β}	–	Rho* (molecule A)
None			

	Gt_{β}	–	Rho (molecule B)
Ionic			
None			
H-bonds			
	Arg52	–	Pro142 (C-II)
	Arg52	–	Lys141 (C-II)
	His54	–	Ser144 (C-II)
	Thr87	–	Thr242 (C-III)
	Asn88	–	Ala241 (C-III)
	Arg129	–	Ala348 (C-term)
	Asn132	–	Ala348 (C-term)
	Asn132	–	Pro347 (C-term)
	Ser334	–	Ser 144 (C-II)
Hydrophobic			
None			

	Gt_{β}	–	Rho (molecule C)
Ionic			
None			
H-bonds			
	Arg42	–	Asn145 (C-II)
	His266	–	Ala348 (C-term)
	Asp267	–	Gln344 (C-term)
	Asn268	–	Ala348 (C-term)
	Asn293	–	Lys141 (C-II)
	Arg304	–	Ala348 (C-term)
	His311	–	Lys141 (C-II)
Hydrophobic			
None			

	Gt_{β}	–	Rho (molecule D)
Ionic			
	Arg46	–	Glu150 (H-IV)
	Arg48	–	Glu150 (H-IV)
	Arg48	–	Glu341 (C-term)
	Arg49	–	Glu341 (C-term)
H-bonds			
	Arg42	–	Arg147 (C-II)
	Arg42	–	Asn145 (C-II)
	Ile43	–	Arg147 (C-II)
	Arg46	–	Arg69 (C-I)
	Arg49	–	Thr340 (C-term)
	Thr50	–	Gln344 (C-term)
Hydrophobic			
None			

	Gt_{γ}	-	Rho (B molecule)
Ionic			
None			
H-bonds			
	Ser74	–	Gln237 (C-III)
	Ser74	–	Lys245 (H-VI)
Hydrophobic			
None			

	Gt_{γ}	–	Rho (D molecule)
Ionic			
	Glu59	–	Lys67 (C-I)
	Lys65	–	Glu341 (C-term)
H-bonds			
	Gly56	–	Lys67 (C-I)
	Pro58	–	Lys67 (C-I)
	Glu59	–	Gln312 (H-8)
	Asp60	–	Thr336 (C-term)
	Asp60	–	Val337 (C-term)
	Lys61	–	Ala333 (C-term)
	Lys65	–	Thr340 (C-term)
	Glu66	–	Ser338 (C-term)
	Lys68	–	Gly324 (C-term)
	Lys68	–	Thr319 (H-8)
Hydrophobic			
None			

	Gt_{α}	–	Gt_{α}
Ionic			
	Asp55	–	Lys206
	Asp154	–	Arg201
	Arg157	–	Asp233
	Asp169	–	Arg201
	Asp324	–	Arg204
	Asp324	–	Lys205
	Asp333	–	Arg253
H-bonds			
	Ile52	–	Tyr254
	Asp55	–	His209
	Tyr57	–	Lys206
	Arg157	–	Glu232
	Val164	–	Arg201
	Glu167	–	Ser202
	Glu167	–	Glu203
	Glu167	–	Lys205
	Glu167	–	Lys206
	Gln326	–	His252
	Lys329	–	Tyr254
Hydrophobic			
	Ile52	–	Ile208
	Phe187	–	Tyr254

[a] Rho dimers: A–B and C–D as shown in Fig. 7. [b] Rho* – activated rhodopsin.

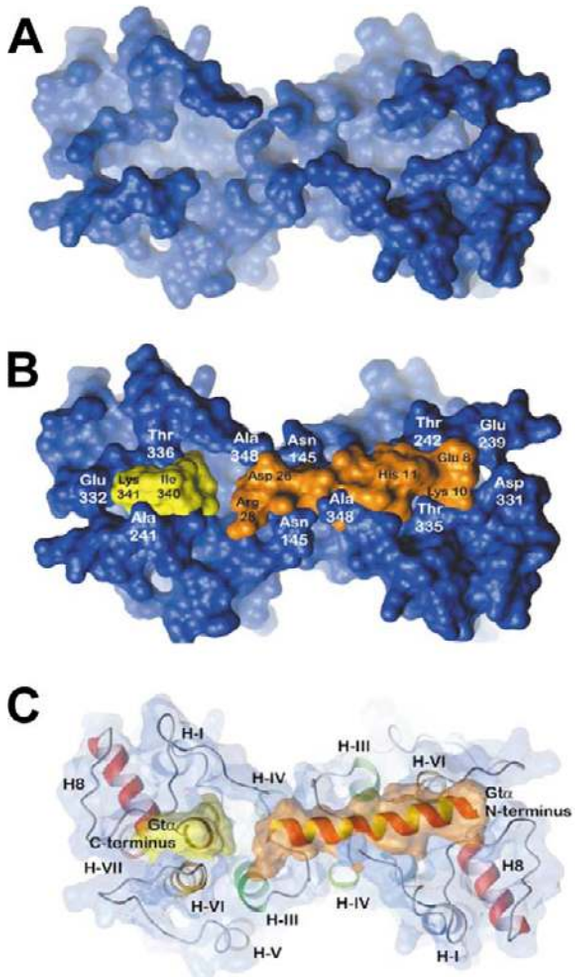

Fig. 9 Top view from the cytoplasmic side of the rhodopsin dimer with and without Gt fragments. (A) Deep cavities on the cytoplasmic surface of the rhodopsin dimer are evident. (B) N-terminal (orange) and C-terminal (yellow) fragments of Gt_{α} docked to the rhodopsin dimer. Original coordinates of the C_{α}-backbone were taken from 1GOT (N-terminal fragment) and 1AQG (C-terminal fragment). No missing N-terminal fragment 1–5 is added to Gt_{α} at this stage. Labels (black for Gt_{α} and white for rhodopsin) denote residues located at the surface facing the viewer. (C) N- and C-termini of Gt_{α} docked to the rhodopsin dimer shown with transparent surfaces. Interacting transmembrane helices of rhodopsin are numbered.

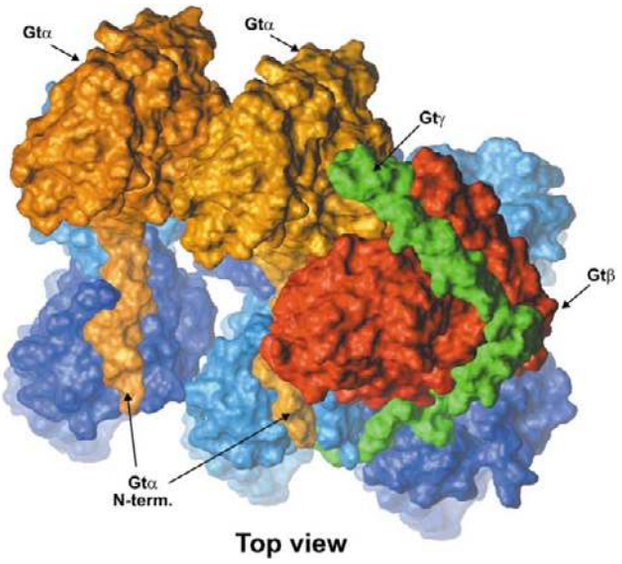

Fig. 10 Three rhodopsin dimers (blue) interacting with two Gt molecules. On the left, two Gt_{α} are depicted after the first $Gt_{\beta\gamma}$ dissociated.

Our modeling study shows that the Gt heterotrimer covers two rhodopsin dimers, and when βγ-subunits dissociate away, another Gt heterotrimer can bind to an adjacent four rhodopsins (two dimers). After dissociation of βγ-subunits from the second Gt, the next Gt can bind to a neighboring rhodopsin tetramer, and so forth (Fig. 10). Both α-subunits not only bind to adjacent rhodopsin dimers, but they also interact with each other. The detailed list of these interactions is given in Table 1. Because of the large volume of the βγ complex, only one Gt can bind when activated rhodopsins lie diagonally in the tetramer. Activation of both rhodopsin molecules in the dimer does not negatively affect Gt binding.

Attractive interactions occur between two Gt_{α} subunits with a range of hydrogen bonds, seven ionic interactions and two hydrophobic interactions. Formation of such interactions can be an additional factor allowing activation of a greater number of Gt molecules on the surface of the rhodopsin paracrystal. Such states, after $Gt_{\beta\gamma}$ is dissociated, are shown in Fig. 11A–C. Two Gt_{α} molecules strongly interact with each other (Table 1) when located on adjacent rhodopsin dimers, suggesting that one Gt_{α} can facilitate binding of a second G protein on an adjacent rhodopsin tetramer.

Based on our model, the activation of one rhodopsin molecule does not prevent activation of any other. There is sufficient space between dimers and between double rows of rhodopsin dimers to accommodate changes in the structure of one activated monomer. Because the main movement during activation is associated with helix VI and this helix is not involved in formation of the dimer interface, the second partner in the dimer is not affected significantly. However, for other GPCRs, for example the angiotensin II receptor and β2-adrenergic receptor, blockade of angiotensin II receptor by antagonist in the heterodimer complex prevents the ability of the agonist activated β2-adrenergic receptor to couple to its G protein.[66] Thus, the conformational changes induced by binding of an antagonist can be passed onto the second receptor by the extracellular loops. This is consistent with our model. The interface between monomers in the rhodopsin dimer consists of the cytoplasmic and extracellular parts. When one rhodopsin is activated (or ligand binds to appropriate GPCR), the extracellular part is changed and passes information about activation/inactivation onto the second monomer (Fig. 2E).

Calculations of the contact area and energy of the complex showed that G-protein does not bind to inactive rhodopsin. The C-terminal region of Gt_{α}, a helix perpendicular to the cytoplasmic surface of the receptor, can enter inactive rhodopsin only partially. This incomplete penetration by the C-terminal region of Gt_{α} leads to elimination of the majority of contacts with the long N-terminal helix of Gt_{α} with the second monomer in the rhodopsin dimer. However, when one rhodopsin in the dimer is active, there is a complementary fit of the long N-terminal helix of Gt_{α} with the cleft on the surface of the adjacent inactive receptor.

Two previous models were proposed to explain how the signal is propagated from the receptors to G proteins leading to nucleotide exchange. A model of G protein activation termed the lever-arm model was proposed first[67,68] in which a monomeric GPCR is a platform for the heterotrimeric Gt. The interface surface between receptors is too small to accommodate all of the regions of Gt that were identified to be involved in the receptor recognition. In this model, a monomeric GPCR brings together N- and C-termini of Gt_{α} opening a cavity to release GDP. Another proposal, by Cherfils and Chabre[69] describes the so called gear-shift model. However, their structural considerations are inadequate, because no geometrical constraints on the distances of the critical parts of G proteins are taken into account.

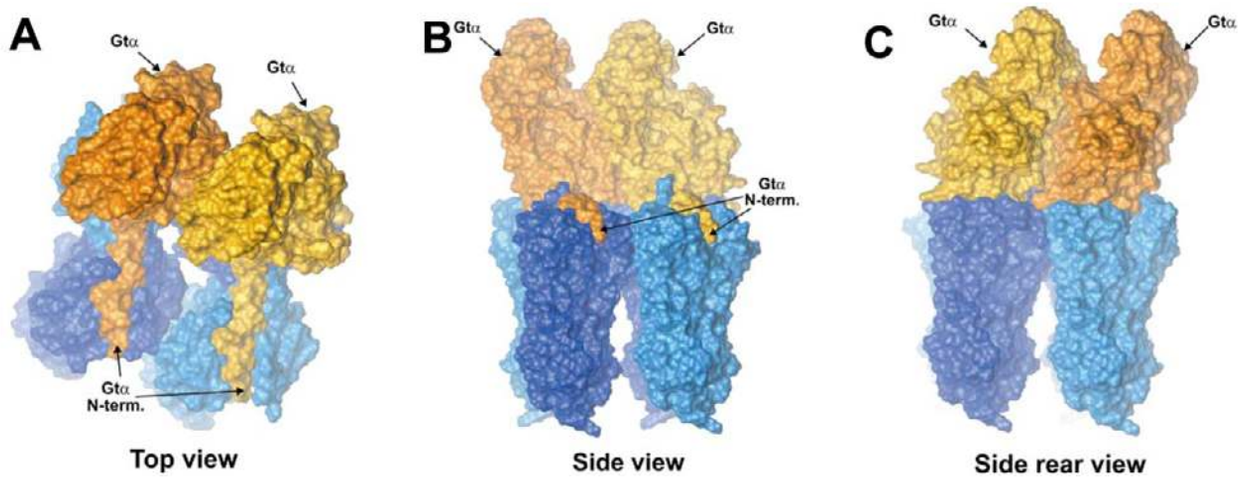

Fig. 11 Complex of two rhodopsin dimers (blue tints) and two α-subunits of Gt (yellow and orange). (A) Top view. (B) Side view. In the foreground, the long N-terminal helices of Gt_{α} are shown. (C) Side rear view of the complex.

Physiological consequences

Oligomerization of GPCRs may cluster these receptors in particular regions of the membranes. This process could be critical for the proper kinetics of GPCR signaling, selectivity, desensitization, and internalization. Hetero-oligomerization may expand the repertoire of GPCRs and their physiological responses, as has been shown for the opioid receptors[29,70,71] and angiotensin receptors.[72–74] Heterodimerization may also enhance signaling and promote cell growth.[75] An abnormality in oligomerization may lead to human conditions such as increased vascular responsiveness to angiotensin II in preeclampsia (eclampsia = seizure during pregnancy)[72] or retinitis pigmentosa, as proposed previously.[38] Receptor maturation during biosynthesis and translocation to the plasma membrane (or ROS membranes for rhodopsin) could also benefit from oligomerization.[76]

As presented in this study, one signaling rhodopsin in the oligomer is needed for productive coupling with Gt (Fig. 7 and 8). This model is consistent with a prototypical single photon response of the photoreceptor cell, in which only a single rhodopsin molecule is photoactivated under dim light conditions.[77] At high illumination levels, the new interactions identified in this study between two Gt_{α} may reduce the number of these subunits available to activate phosphodiesterase. In detergent solutions, it is possible that a single activated rhodopsin interacts with Gt, although $Gt_{\beta\gamma}$ subunits will not interact with the receptor at the same time.

Heterodimerization of GPCRs may lead to many combinatorial possibilities with novel pharmacological properties.[34] The overall structures of G-proteins and GPCRs, and the mechanism of action appear to be similar.[8,20] Thus, these observations imply a common mechanism of docking of G-proteins onto tetramers formed by even different receptors. The fundamental observation is that G-protein binds to a dimer, while the second dimer is only a docking platform.

Proteins interacting with GPCRs evolved to accommodate the multimeric structures. The case of Gt has been presented here, and the bipartite structure of arrestin also fits well with the dimer of rhodopsin[38] (see also ref. 78). The crystal structure of G protein-coupled receptor kinase, GRK2,[79] is also in structural agreement with the oligomeric structures of GPCRs.[84] These properties may be important for optimal responses to a wide range of agonist concentrations and reciprocal receptor desensitization at higher concentrations of the agonist.

Conclusions

Here, we present a concept of the interaction between a heterotrimeric G protein and its receptor that builds on the crystal structures of individual proteins, membrane arrangements, geometrical constraints, and the lipid environment. We have chosen the visual system because the crystal structures of rhodopsin and Gt have been elucidated. Moreover, we recently revealed the oligomeric structure of rhodopsin in native disc membranes by AFM.[37–40] This arrangement was in agreement with many indirect observations in the GPCR field.[39] The shapes and sizes of rhodopsin and Gt impose major constraints on how the receptor interacts with its cognate G protein, a feature that is not considered in many peptide-competition, biophysical or site-specific mutagenesis studies of GPCRs and G proteins. Our modeling suggests that the classic view of GPCR signaling of oligomers of G protein and the receptors expressed by Rodbell and co-workers[80,81] is consistent with the structural evidence. Verification of our detailed model and its further fine tuning await results from experimental approaches. We find it encouraging that our model is in good agreement with *trans*-activation of family A GPCRs using fusion proteins between receptors and G proteins[82] and the identified pentameric complex between dimeric leukotriene B4 receptor BLT1 and heterotrimeric Gi.[65]

Abbreviations

AFM, atomic force microscopy (microscope); C-I, cytoplasmic loop I; EM, electron microscopy; GPCR, G protein-coupled receptor; Gt, transducin (rod photoreceptor-specific G protein); H-I, helix I; PDB, Protein Data Bank; ROS, rod outer segment(s).

Acknowledgements

We would like to thank Dr. K. Ridge, Dr. Ron Stenkamp, Dr. John Tesmer and Dr. W. Baehr for comments on the manuscript. This research was supported in part by US Public Health Service grants EY01730 and EY08061 from the National Eye Institute, National Institutes of Health, Bethesda, MD, an unrestricted Grant from Research to Prevent Blindness, Inc. (RPB), New York, NY to the Department of Ophthalmology at the University of Washington, and grants from the E. K. Bishop Foundation, Foundation Fighting Blindness, and Jim and Jane Lea Research Fund. A. E. acknowledges support by the Swiss National Research Foundation, the M. E. Müller Foundation, the Swiss National Center of Competence in Research (NCCR) 'Structural Biology', and the NCCR 'Nanoscale Science'. This study was supported by funds from Polish State Committee for Scientific Research 2003–2006 research project 3P05F02625.

References

1 U. Gether, Uncovering molecular mechanisms involved in activation of G protein-coupled receptors, *Endocr. Rev.*, 2000, **21**, 90–113.
2 J. A. Ballesteros, L. Shi and J. A. Javitch, Structural mimicry in G protein-coupled receptors: implications of the high-resolution structure of rhodopsin for structure-function analysis of rhodopsin-like receptors, *Mol. Pharmacol.*, 2001, **60**, 1–19.
3 T. Mirzadegan, G. Benko, S. Filipek and K. Palczewski, Sequence analyses of G-protein-coupled receptors: similarities to rhodopsin, *Biochemistry*, 2003, **42**, 2759–2767.
4 K. L. Pierce, R. T. Premont and R. J. Lefkowitz, Seven-transmembrane receptors, *Nat. Rev. Mol. Cell Biol.*, 2002, **3**, 639–650.
5 S. Filipek, R. E. Stenkamp, D. C. Teller and K. Palczewski, G protein-coupled receptor rhodopsin: a prospectus, *Annu. Rev. Physiol.*, 2003, **65**, 851–879.
6 A. Polans, W. Baehr and K. Palczewski, Turned on by Ca^{2+}! The physiology and pathology of Ca^{2+}-binding proteins in the retina, *Trends Neurosci.*, 1996, **19**, 547–554.
7 T. Okada and K. Palczewski, Crystal structure of rhodopsin: implications for vision and beyond, *Curr. Opin. Struct. Biol.*, 2001, **11**, 420–426.
8 T. Okada, O. P. Ernst, K. Palczewski and K. P. Hofmann, Activation of rhodopsin: new insights from structural and biochemical studies, *Trends Biochem. Sci.*, 2001, **26**, 318–324.
9 K. Palczewski, T. Kumasaka, T. Hori, C. A. Behnke, H. Motoshima, B. A. Fox, I. Le Trong, D. C. Teller, T. Okada, R. E. Stenkamp, M. Yamamoto and M. Miyano, Crystal structure of rhodopsin: a G protein-coupled receptor, *Science*, 2000, **289**, 739–745.
10 D. C. Teller, T. Okada, C. A. Behnke, K. Palczewski and R. E. Stenkamp, Advances in determination of a high-resolution three-dimensional structure of rhodopsin, a model of G-protein-coupled receptors (GPCRs), *Biochemistry*, 2001, **40**, 7761–7772.
11 S. Filipek, D. C. Teller, K. Palczewski and R. Stenkamp, The crystallographic model of rhodopsin and its use in studies of other G protein-coupled receptors, *Annu. Rev. Biophys. Biomol. Struct.*, 2003, **32**, 375–397.
12 J. Sondek, A. Bohm, D. G. Lambright, H. E. Hamm and P. B. Sigler, Crystal structure of a G-protein βγ dimer at 2.1 Å resolution, *Nature*, 1996, **379**, 369–374.
13 J. J. Tesmer, R. K. Sunahara, A. G. Gilman and S. R. Sprang, Crystal structure of the catalytic domains of adenylyl cyclase in a complex with GsαGTPγS, *Science*, 1997, **278**, 1907–1916.
14 D. G. Lambright, J. P. Noel, H. E. Hamm and P. B. Sigler, Structural determinants for activation of the α-subunit of a heterotrimeric G protein, *Nature*, 1994, **369**, 621–628.
15 D. G. Lambright, J. Sondek, A. Bohm, N. P. Skiba, H. E. Hamm and P. B. Sigler, The 2.0 Å crystal structure of a heterotrimeric G protein, *Nature*, 1996, **379**, 311–319.
16 D. E. Coleman, A. M. Berghuis, E. Lee, M. E. Linder, A. G. Gilman and S. R. Sprang, Structures of active conformations of $Gi\alpha_1$ and the mechanism of GTP hydrolysis, *Science*, 1994, **265**, 1405–1412.
17 C. Kleuss, A. S. Raw, E. Lee, S. R. Sprang and A. G. Gilman, Mechanism of GTP hydrolysis by G-protein α subunits, *Proc. Natl. Acad. Sci. USA*, 1994, **91**, 9828–9831.
18 M. A. Wall, D. E. Coleman, E. Lee, J. A. Iniguez-Lluhi, B. A. Posner, A. G. Gilman and S. R. Sprang, The structure of the G protein heterotrimer $Gi\alpha_1\beta_1\gamma_2$, *Cell*, 1995, **83**, 1047–1058.
19 D. E. Coleman and S. R. Sprang, Structure of $Gi\alpha_1$.GppNHp, autoinhibition in a Gα protein-substrate complex, *J. Biol. Chem.*, 1999, **274**, 16669–16672.
20 K. D. Ridge, N. G. Abdulaev, M. Sousa and K. Palczewski, Phototransduction: crystal clear, *Trends Biochem. Sci.*, 2003, **28**, 479–487.
21 J. A. Hirsch, C. Schubert, V. V. Gurevich and P. B. Sigler, The 2.8 Å crystal structure of visual arrestin: a model for arrestin's regulation, *Cell*, 1999, **97**, 257–269.
22 J. Granzin, U. Wilden, H. W. Choe, J. Labahn, B. Krafft and G. Buldt, X-ray crystal structure of arrestin from bovine rod outer segments, *Nature*, 1998, **391**, 918–921.
23 S. K. Milano, H. C. Pace, Y. M. Kim, C. Brenner and J. L. Benovic, Scaffolding functions of arrestin-2 revealed by crystal structure and mutagenesis, *Biochemistry*, 2002, **41**, 3321–3328.
24 K. Palczewski, Structure and functions of arrestins, *Protein Sci.*, 1994, **3**, 1355–1361.
25 D. C. Teller, R. E. Stenkamp and K. Palczewski, Evolutionary analysis of rhodopsin and cone pigments: connecting the three-dimensional structure with spectral tuning and signal transfer, *FEBS Lett.*, 2003, **555**, 151–159.
26 G. Milligan, Oligomerisation of G-protein-coupled receptors, *J. Cell Sci*, 2001, **114**, 1265–1271.
27 S. R. George, B. F. O'Dowd and S. P. Lee, G-protein-coupled receptor oligomerization and its potential for drug discovery, *Nat. Rev. Drug Discovery*, 2002, **1**, 808–820.
28 S. Angers, A. Salahpour and M. Bouvier, Dimerization: an emerging concept for G protein-coupled receptor ontogeny and function, *Annu. Rev. Pharmacol. Toxicol.*, 2002, **42**, 409–435.
29 C. D. Rios, B. A. Jordan, I. Gomes and L. A. Devi, G-protein-coupled receptor dimerization: modulation of receptor function, *Pharmacol. Ther.*, 2001, **92**, 71–87.
30 S. P. Lee, B. F. O'Dowd and S. R. George, Homo- and hetero-oligomerization of G protein-coupled receptors, *Life Sci.*, 2003, **74**, 173–180.
31 G. Milligan, D. Ramsay, G. Pascal and J. J. Carrillo, GPCR dimerisation, *Life Sci.*, 2003, **74**, 181–188.
32 B. Moepps and L. Fagni, Mont Sainte-Odile: a sanctuary for GPCRs. Confidence on signal transduction of G-protein-coupled receptors, *EMBO Rep.*, 2003, **4**, 237–243.
33 M. Bai, Dimerization of G-protein-coupled receptors: roles in signal transduction, *Cell Signal.*, 2004, **16**, 175–186.
34 S. Terrillon and M. Bouvier, Roles of G-protein-coupled receptor dimerization, *EMBO Rep.*, 2004, **5**, 30–34.
35 G. E. Breitwieser, G protein-coupled receptor oligomerization: implications for G protein activation and cell signaling, *Circ. Res.*, 2004, **94**, 17–27.
36 C. Bissantz, Conformational changes of G protein-coupled receptors during their activation by agonist binding, *J. Recept. Signal. Transduct. Res.*, 2003, **23**, 123–153.
37 D. Fotiadis, Y. Liang, S. Filipek, D. A. Saperstein, A. Engel and K. Palczewski, Atomic-force microscopy: rhodopsin dimers in native disc membranes, *Nature*, 2003, **421**, 127–128.
38 Y. Liang, D. Fotiadis, S. Filipek, D. A. Saperstein, K. Palczewski and A. Engel, Organization of the G protein-coupled receptors rhodopsin and opsin in native membranes, *J. Biol. Chem.*, 2003, **278**, 21655–21662.
39 D. Fotiadis, Y. Liang, S. Filipek, D. A. Saperstein, A. Engel and K. Palczewski, The G protein-coupled receptor rhodopsin in the native membrane, *FEBS Lett.*, 2004, in press.
40 D. Fotiadis, Y. Liang, S. Filipek, D. A. Saperstein, A. Engel and K. Palczewski, Biophysics (communication arising): Reply: Is rhodopsin dimeric in native retinal rods?, *Nature*, 2003, **426**, 31.
41 M. Chabre, R. Cone and H. Saibil, Biophysics: is rhodopsin dimeric in native retinal rods?, *Nature*, 2003, **426**, 30–31.
42 O. Fritze, S. Filipek, V. Kuksa, K. Palczewski, K. P. Hofmann and O. P. Ernst, Role of the conserved NPxxY(x)5,6F motif in the rhodopsin ground state and during activation, *Proc. Natl. Acad. Sci. USA*, 2003, **100**, 2290–2295.
43 N. M. Giusto, S. J. Pasquare, G. A. Salvador, P. I. Castagnet, M. E. Roque and M. G. Ilincheta de Boschero, Lipid metabolism in vertebrate retinal rod outer segments, *Prog. Lipid Res.*, 2000, **39**, 315–391.
44 L. Saiz and M. L. Klein, Structural properties of a highly polyunsaturated lipid bilayer from molecular dynamics simulations, *Biophys. J.*, 2001, **81**, 204–216.
45 H. E. Hamm, The many faces of G protein signaling, *J. Biol. Chem.*, 1998, **273**, 669–672.
46 O. G. Kisselev, J. Kao, J. W. Ponder, Y. C. Fann, N. Gautam and G. R. Marshall, Light-activated rhodopsin induces structural binding motif in G protein α subunit, *Proc. Natl. Acad. Sci. USA*, 1998, **95**, 4270–4275.
47 M. H. Elliott, S. J. Fliesler and A. J. Ghalayini, Cholesterol-dependent association of caveolin-1 with the transducin alpha subunit in bovine photoreceptor rod outer segments: disruption by cyclodextrin and guanosine 5′-*O*-(3-thiotriphosphate), *Biochemistry*, 2003, **42**, 7892–7903.
48 K. S. Nair, N. Balasubramanian and V. Z. Slepak, Signal-dependent translocation of transducin, RGS9-1-Gβ5L complex, and arrestin to detergent-resistant membrane rafts in photoreceptors, *Curr. Biol.*, 2002, **12**, 421–425.
49 N. Balasubramanian and V. Z. Slepak, Light-mediated activation of Rac-1 in photoreceptor outer segments, *Curr. Biol.*, 2003, **13**, 1306–1310.
50 K. Seno, M. Kishimoto, M. Abe, Y. Higuchi, M. Mieda, Y. Owada, W. Yoshiyama, H. Liu and F. Hayashi, Light- and guanosine 5′-3-*O*-(thio)triphosphate-sensitive localization of a G protein and its effector on detergent-resistant membrane rafts in rod photoreceptor outer segments, *J. Biol. Chem.*, 2001, **276**, 20813–20816.
51 S. S. Karnik and H. G. Khorana, Assembly of functional rhodopsin requires a disulfide bond between cysteine residues 110 and 187, *J. Biol. Chem.*, 1990, **265**, 17520–17524.
52 L. Shi and J. A. Javitch, The second extracellular loop of the

dopamine D2 receptor lines the binding-site crevice, *Proc. Natl. Acad. Sci. USA*, 2004, **101**, 440–445.
53 W. L. Stone, C. C. Farnsworth and E. A. Dratz, A reinvestigation of the fatty acid content of bovine, rat and frog retinal rod outer segments, *Exp. Eye Res.*, 1979, **28**, 387–397.
54 P. D. Calvert, V. I. Govardovskii, N. Krasnoperova, R. E. Anderson, J. Lem and C. L. Makino, Membrane protein diffusion sets the speed of rod phototransduction, *Nature*, 2001, **411**, 90–94.
55 J. Sondek, D. G. Lambright, J. P. Noel, H. E. Hamm and P. B. Sigler, GTPase mechanism of Gproteins from the 1.7 Å crystal structure of transducin α-GDP-AIF^{-4}, *Nature*, 1994, **372**, 276–279.
56 H. E. Hamm, Molecular interactions between the photoreceptor G protein and rhodopsin, *Cell Mol. Neurobiol.*, 1991, **11**, 563–578.
57 H. E. Hamm and A. Gilchrist, Heterotrimeric G proteins, *Curr. Opin. Cell Biol.*, 1996, **8**, 189–196.
58 S. Acharya, Y. Saad and S. S. Karnik, Transducin-α C-terminal peptide binding site consists of C–D and E–F loops of rhodopsin, *J. Biol. Chem.*, 1997, **272**, 6519–6524.
59 K. Cai, Y. Itoh and H. G. Khorana, Mapping of contact sites in complex formation between transducin and light-activated rhodopsin by covalent crosslinking: use of a photoactivatable reagent, *Proc. Natl. Acad. Sci. USA*, 2001, **98**, 4877–4882.
60 Y. Itoh, K. Cai and H. G. Khorana, Mapping of contact sites in complex formation between light-activated rhodopsin and transducin by covalent crosslinking: use of a chemically preactivated reagent, *Proc. Natl. Acad. Sci. USA*, 2001, **98**, 4883–4887.
61 O. P. Ernst, C. K. Meyer, E. P. Marin, P. Henklein, W. Y. Fu, T. P. Sakmar and K. P. Hofmann, Mutation of the fourth cytoplasmic loop of rhodopsin affects binding of transducin and peptides derived from the carboxyl-terminal sequences of transducin α and γ subunits, *J. Biol. Chem.*, 2000, **275**, 1937–1943.
62 E. P. Marin, A. G. Krishna, T. A. Zvyaga, J. Isele, F. Siebert and T. P. Sakmar, The amino terminus of the fourth cytoplasmic loop of rhodopsin modulates rhodopsin-transducin interaction, *J. Biol. Chem.*, 2000, **275**, 1930–1936.
63 E. Kostenis, F. Y. Zeng and J. Wess, Functional characterization of a series of mutant G protein αq subunits displaying promiscuous receptor coupling properties, *J. Biol. Chem.*, 1998, **273**, 17886–17892.
64 R. Arimoto, O. G. Kisselev, G. M. Makara and G. R. Marshall, Rhodopsin-transducin interface: studies with conformationally constrained peptides, *Biophys. J.*, 2001, **81**, 3285–3293.
65 J. L. Baneres and J. Parello, Structure-based analysis of GPCR function: evidence for a novel pentameric assembly between the dimeric leukotriene B4 receptor BLT1 and the G-protein, *J. Mol. Biol.*, 2003, **329**, 815–829.
66 L. Barki-Harrington, L. M. Luttrell and H. A. Rockman, Dual inhibition of beta-adrenergic and angiotensin II receptors by a single antagonist: a functional role for receptor-receptor interaction *in vivo*, *Circulation*, 2003, **108**, 1611–1618.
67 T. Iiri, Z. Farfel and H. R. Bourne, G-protein diseases furnish a model for the turn-on switch, *Nature*, 1998, **394**, 35–38.
68 P. Rondard, T. Iiri, S. Srinivasan, E. Meng, T. Fujita and H. R. Bourne, Mutant G protein α subunit activated by Gβγ: a model for receptor activation?, *Proc. Natl. Acad. Sci. USA*, 2001, **98**, 6150–6155.
69 J. Cherfils and M. Chabre, Activation of G-protein Gα subunits by receptors through Gα–Gβ and Gα–Gγ interactions, *Trends Biochem. Sci.*, 2003, **28**, 13–17.
70 I. Gomes, B. A. Jordan, A. Gupta, C. Rios, N. Trapaidze and L. A. Devi, G protein coupled receptor dimerization: implications in modulating receptor function, *J. Mol. Med.*, 2001, **79**, 226–242.
71 B. A. Jordan and L. A. Devi, G-protein-coupled receptor heterodimerization modulates receptor function, *Nature*, 1999, **399**, 697–700.
72 S. AbdAlla, H. Lother, A. el Massiery and U. Quitterer, Increased AT(1) receptor heterodimers in preeclampsia mediate enhanced angiotensin II responsiveness, *Nat. Med.*, 2001, **7**, 1003–1009.
73 S. AbdAlla, H. Lother, A. M. Abdel-tawab and U. Quitterer, The angiotensin II AT2 receptor is an AT1 receptor antagonist, *J. Biol. Chem.*, 2001, **276**, 39721–39726.
74 S. AbdAlla, H. Lother and U. Quitterer, AT1–receptor heterodimers show enhanced G-protein activation and altered receptor sequestration, *Nature*, 2000, **407**, 94–98.
75 Z. J. Cheng, K. G. Harikumar, E. L. Holicky and L. J. Miller, Heterodimerization of type A and B cholecystokinin receptors enhance signaling and promote cell growth, *J. Biol. Chem.*, 2003, **278**, 52972–52979.
76 M. C. Overton, S. L. Chinault and K. J. Blumer, Oligomerization, biogenesis, and signaling is promoted by a Glycophorin A-like dimerization motif in transmembrane domain 1 of a yeast G protein-coupled receptor, *J. Biol. Chem.*, 2003, **278**, 49369–49377.
77 D. Baylor, How photons start vision, *Proc. Natl. Acad. Sci. USA*, 1996, **93**, 560–565.
78 S. A. Vishnivetskiy, M. M. Hosey, J. L. Benovic and V. V. Gurevich, Mapping the arrestin–receptor interface: Structural elements responsible for receptor specificity of arrestin proteins, *J. Biol. Chem.*, 2004, **279**, 1262–1268.
79 D. T. Lodowski, J. A. Pitcher, W. D. Capel, R. J. Lefkowitz and J. J. Tesmer, Keeping G proteins at bay: a complex between G protein-coupled receptor kinase 2 and Gβγ, *Science*, 2003, **300**, 1256–1262.
80 M. Rodbell, Nobel Lecture. Signal transduction: evolution of an idea, *Biosci. Rep.*, 1995, **15**, 117–133.
81 W. Schlegel, E. S. Kempner and M. Rodbell, Activation of adenylate cyclase in hepatic membranes involves interactions of the catalytic unit with multimeric complexes of regulatory proteins, *J. Biol. Chem.*, 1979, **254**, 5168–5176.
82 J. J. Carrillo, J. Pediani and G. Milligan, Dimers of class A G protein-coupled receptors function *via* agonist-mediated *trans*-activation of associated G proteins, *J. Biol. Chem.*, 2003, **278**, 42578–42587.
83 P. K. Brown, I. R. Gibbons and G. Wald, The visual cells and visual pigment of the mudpuppy, necturus, *J. Cell Biol.*, 1963, **19**, 79–106.
84 S. Filipek *et al.*, in preparation.